Geo-Marine Letters (2001) 21: 168–175
DOI 10.1007/s003670100080

Sonja Schulte · Peter J. Müller

Variations of sea surface temperature and primary productivity during Heinrich and Dansgaard-Oeschger events in the northeastern Arabian Sea

Received: 8 January 2001 / Revision accepted: 10 August 2001 / Published online: 5 October 2001

Abstract Sea surface temperatures (SST) and primary productivities have been reconstructed for the northeastern Arabian Sea during the past 65,000 years, using C_{37}-alkenones. Comparison of this SST record with $\delta^{18}O$ from Greenland ice core GISP2 shows striking similarities, indicating an apparent linkage between the climate of the Arabian Sea with that of the northern North Atlantic, most probably via atmospheric and/or oceanic circulation. These rapid SST changes are in the long term overlain by insolation changes at 30°N.

Introduction

During the past 100,000 years, Heinrich events (HEs) and Dansgaard-Oeschger (D-O) cycles have been the dominant signal of climate variability over Greenland and the northern North Atlantic (Heinrich 1988; Johnsen et al. 1992; Bond et al. 1993; Dansgaard et al. 1993). Time equivalents of these cycles and events have been reported in a variety of records (marine, lacustrine, terrestrial) in both hemispheres all over the world (e.g., Bender et al. 1994; Thouveny et al. 1994; Porter and An 1995; Behl and Kennett 1996; Schulz et al. 1998; Cacho et al. 1999; Rühlemann et al. 1999; Schulte et al. 1999; Wang and Sarnthein 1999; Leuschner and Sirocko 2000; Bard et al. 2000).

A close coupling between the North Atlantic and monsoon climates was suggested by several studies from the Arabian Sea (e.g., von Rad et al. 1995; Sirocko et al. 1996; Reichart et al. 1998; Schulz et al. 1998; Schulte et al. 1999; Leuschner and Sirocko 2000) and China (Porter and An 1995; Wang and Sarnthein 1999; Fang et al. 1999; Lin et al. 1999; Zhou et al. 1999). Most of these studies dealt with parameters coupled somehow to the monsoon (e.g., organic carbon, biomarkers, grain size, cadmium, barium, Sr/Ca ratio, carbonate), the main climatic feature of this region. However, the mechanisms coupling the climates of both these regions are still poorly understood.

Sea surface temperature (SST) is a good and easily determined measure of modern climatic conditions. SST is probably the most important parameter for describing the conditions of past oceans, and is essential for climate modeling. For this reason, estimation of past SST in the northeastern Arabian Sea is crucial to better understand how the low-latitude monsoonal climate is coupled to that of the high northern latitudes. Recently, a high-resolution temperature record for the northeastern Arabian Sea during the late Holocene was published (Doose-Rolinski et al. 2001). Here, we present the first late-Quaternary SST record from the northeastern Arabian Sea, using the alkenone method (see Bard 2001 for a detailed comparison of alkenone estimates with other paleotemperature proxies) with sufficient temporal resolution permitting comparison with the millennial-scale events recorded in Greenland ice cores.

Atmospheric and oceanographic setting

The modern Arabian Sea is characterized by the seasonal variability of the monsoon wind system, with a strong and humid southwest (SW) monsoon during the summer (June–September) which is driven by a strong pressure gradient between the Tibetan low-pressure cell and a belt of high pressure over the Southern Ocean. The modern SW monsoon is driven mainly by differential ocean-land heating and tropospheric latent heating (Clemens et al. 1991). The winter season (December–February) is characterized by the moderate and dry northeast (NE) monsoon which blows from a strong high-pressure cell above central Asia to the region of low pressure associated with the intertropical convergence zone at ~10°S.

S. Schulte (✉) · P.J. Müller
University of Bremen, Geosciences,
P.O. Box 330 440, 28334 Bremen, Germany
E-mail: sschulte@uni-bremen.de

The SW monsoon causes an intense upwelling off Oman and Somalia resulting in high primary productivity (Wyrtki 1973; Pickard and Emery 1982; Bearman 1991; Brock et al. 1992). By contrast, the NE monsoon causes no upwelling, but sets up the stage for convective mixing due to surface water cooling (Madhupratap et al. 1996).

An important feature of the Arabian Sea is the exceptionally broad and stable mid-water oxygen minimum zone (OMZ) between 200 and ~1,100 m water depths (Wyrtki 1973; von Rad et al. 1995), maintained by various factors including oxygen consumption by organic matter decay and supply of oxygen-depleted intermediate waters from the south (for a detailed description of the hydrography see Swallow 1984; Olson et al. 1993; Schulte et al. 1999; and references therein). Recently, it has been demonstrated that the stability of the OMZ varied in concert with the D-O cycles and HEs in Greenland ice cores (Reichart et al. 1998; Schulz et al. 1998; Schulte et al. 1999).

The high primary productivity observed in the northeastern Arabian Sea is most likely caused by the northeastward drift (Fig. 1) of nutrient-rich surface waters, with a high standing stock of biomass, from Oman to the Pakistan margin, forced by the strong SW monsoonal winds (Schulz et al. 1996, 1998; Andruleit et al. 2000). The slight enhancement of productivity at the end of the NE monsoon, which coincides with a decrease of SST, could be explained by wind-induced deepening of the mixed layer which injects nutrients to the surface (Fig. 2d; Madhupratap et al. 1996). This explanation is consistent with the results of Prahl et al. (2000) who observed a simultaneous enhancement of alkenone flux and deepening of the mixed layer in the central Arabian Sea.

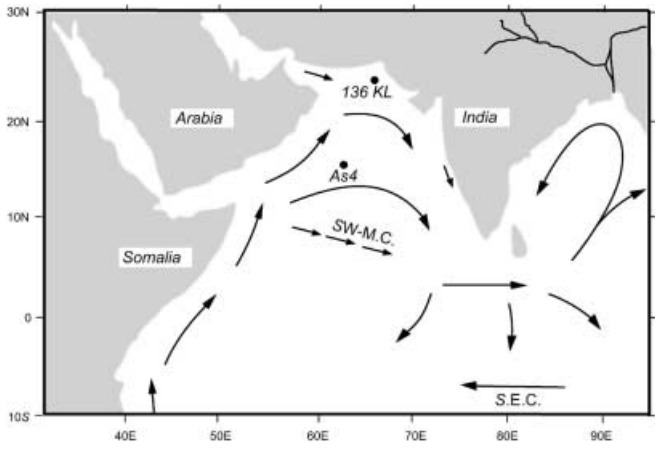

Fig. 1 Map of the Arabian Sea showing the location of core 136 KL and that of sediment trap AS4 (Prahl et al. 2000). Arrows indicate the oceanic surface circulation during the SW monsoon. *SW-M.C.* Southwest monsoon current; *S.E.C.* south equatorial current

Study site

Piston core 136 KL was obtained during the SONNE 90 cruise in 1993 (23°7.34′N, 66°29.83′E, 568 m water depth, Fig. 1; von Rad et al. 1995) from within the modern OMZ on the continental slope off Pakistan. At the location of core 136 KL, highest primary productivity is observed in July when wind speed reaches its maximum during the SW monsoon, as indicated by satellite observations (Antoine et al. 1996; Fig. 2a). The constantly high SST (27–29 °C, Fig. 2e) during the SW monsoon points to the absence of upwelling in this area, as suggested by Schulz et al. (1996, 1998). A supply of nutrients due to wind-induced vertical mixing can also

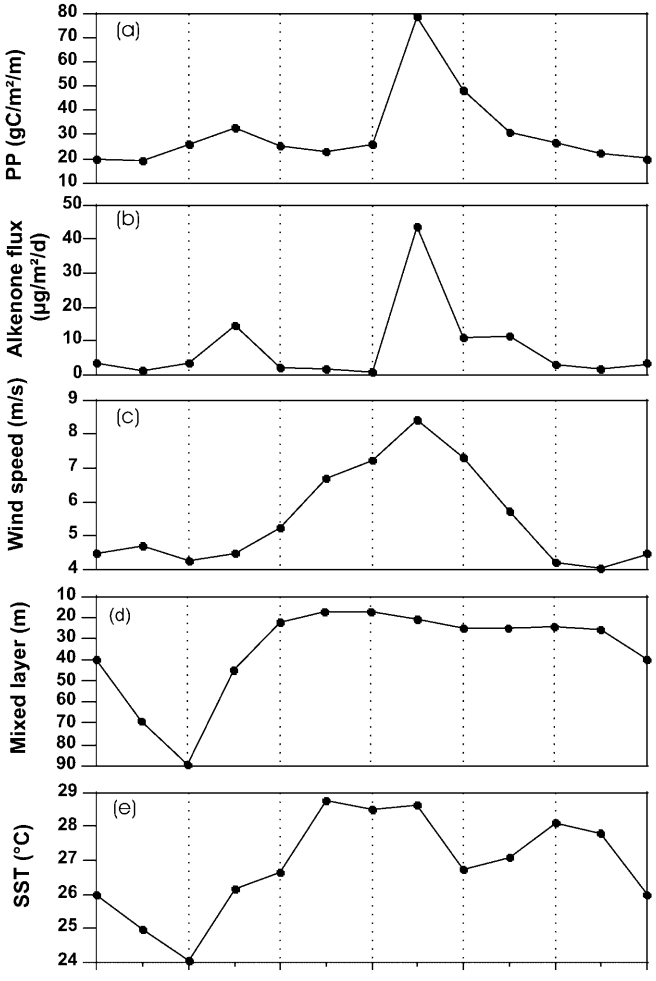

Fig. 2 (modified after Schulte et al. 1999). **a** Annual variability of primary productivity (*PP*) at site 136 KL (after Antoine et al. 1996). **b** Monthly mean alkenone flux at sediment trap AS4 (after Prahl et al. 2000). **c** Annual variability of total wind speed at site 136 KL (COADS Atlas). **d** Annual variability of mixed layer depth at site 136 KL (IGOSS Atlas). **e** Annual variability of sea surface temperature (*SST*) at site 136 KL (23°7.34′N, 66°29.83′E; Levitus Atlas). The COADS Atlas, IGOSS Atlas and Levitus Atlas data were extracted from the web site http://ingrid.ldgo.columbia.edu. The resolution of the IGOSS Atlas is rather coarse (2° latitude, 5° longitude) Therefore, we averaged the four nearest values available (22°N, 65°E; 22°N, 70°E; 24°N, 65°E; 24°N, 70°E)

be excluded at site 136 KL because no deepening of the mixed-layer depth is observed (Fig. 2d; Banse 1984), in contrast to the central Arabian Sea where deepening of the mixed layer also takes place during the SW monsoon (Prahl et al. 2000). The lowest SST occurs in February (24 °C, Fig. 2e), induced by the NE monsoon which originates from the snow-covered Asian mountains and strongly cools the northern Arabian Sea (Wyrtki 1973).

Materials and methods

Sediment samples were collected from piston core 136 KL immediately after recovery or from a subcore which was stored at 4 °C. A detailed description of the extraction method can be found elsewhere (Benthien and Müller 2000; Budziak et al. 2000). Briefly, alkenones were extracted from 1- to 3-g aliquots of freeze-dried and homogenized sediments, using UP 200H ultrasonic disrupter probes (200 W, amplitude 0.5, pulse 0.5) and successively less polar mixtures of methanol and dichloromethane (CH_3OH, CH_3OH:CH_2Cl_2 (1:1), CH_2Cl_2), each for 3 min. The three extracts were combined, washed with demineralized water to remove sea salt and methanol, dried over $NaSO_4$, and concentrated under N_2. The concentrated extracts were purified by passing them over a silica gel cartridge (Varian Bond Elut; 1 cm^3 100 mg^{-1}), and then saponified. For saponification 0.3 ml of 0.1 M KOH in methanol:water (90:10) was added to the extract and heated at 80 °C in a capped vial for 2 h. After cooling the alkenone-containing fraction was obtained by partitioning into *n*-hexane and then concentrated.

The analytical conditions of gas chromatography are described elsewhere (Benthien and Müller 2000). Analytical precision was better than 0.01 $U^{k'}_{37}$ units (± 0.3 °C), based on replicate extractions and injections of selected samples and laboratory internal reference sediments. SSTs were estimated from the relative composition of C_{37} unsaturated alkenones ($U^{k'}_{37}$-index; Brassell et al. 1986), using the global core top calibration of Müller et al. (1998; $U^{k'}_{37} = 0.033T + 0.044$). This equation relates $U^{k'}_{37}$ to mean annual SST between 0 and 28 °C.

Results

Sea surface temperatures

A detailed $\delta^{18}O$ stratigraphy was established using the surface-dwelling planktonic Foraminifera *Globigerinoides ruber* and by AMS ^{14}C dating of the 16.5-m-long piston core, spanning the last 65,000 years (Schulz et al. 1998; H. Schulz, personal communication). Schulz et al. (1998) reported a remarkable similarity between the TOC record, or more precisely a crude approximation based on the sediment color (gray scale) of core 136 KL and $\delta^{18}O$ of the Greenland ice core GISP2 (Fig. 3b). The alkenone record studied here has a lower resolution than the continuous gray scale of Schulz et al. (1998), but previously measured and reported TOC values match very closely with the gray-scale-based TOC record, so that most climatic events could be identified (Schulte et al. 1999).

Temperature fluctuations of up to 4 °C are observed during the last 65,000 years in core 136 KL (Fig. 3c). The Holocene is characterized by temperatures between 27 and 28 °C, consistent with Holocene temperatures reported in a variety of cores from the tropical Indian Ocean (25.2–28.3 °C; Sonzogni et al. 1998). Between the last glacial maximum and the Holocene a SST difference of about 3.5 °C is observed, which is greater than the values reported by Sonzogni et al. (1998; 1.5–2.5 °C).

The last deglaciation is characterized by an abrupt 2.5 °C warming at about 15 ka B.P., followed by a temperature plateau lasting approximately 3,000 years. At about 12 ka B.P., a cooling event is observed which is correlated with the Younger Dryas (YD). However, the temperature reversal does not correspond to a return to full glacial conditions as in the case of Greenland records (Fig. 3a). The second part of the deglaciation is more gradual, exhibiting a warming of 2 °C from 12 ka B.P. up to a present-day value of 27.5 °C. The glacial period between 65 and 15 ka B.P. is characterized by rapid temperature variations between 23.5 and about 26 °C.

Alkenone enrichment and mass accumulation rates

To evaluate qualitative changes in primary productivity during the last 65,000 years in the northeastern Arabian Sea, we used C_{37}-alkenone abundance which has been suggested to be a reliable qualitative proxy for paleoproductivity (Rostek et al. 1997; Schubert et al. 1998; Villanueva et al. 1998; Schulte et al. 1999; Budziak et al. 2000). The usefulness of C_{37}-alkenone abundance as a productivity proxy was recently confirmed by a sediment trap study (Fig. 2b; Prahl et al. 2000). The long-chain alkenones are produced by coccolithophorides of the class *Haptophytes* (Conte and Eglinton 1993; Volkman et al. 1995), one of the most important contributors to primary productivity in the study area (Banse 1994). To account for a possible effect of mineral dilution we also estimated the mass accumulation rate (MAR) of the alkenones, which is equal to the product of sedimentation rate, alkenone content and dry bulk density (0.75 g cm^{-3}, assumed to be constant). In core 136 KL total C_{37}-alkenone contents vary between 0.4 and about 30 μg g^{-1} dry sediment, and the MAR between 100 and about 600 μg cm^{-2} 1,000 $year^{-1}$, in general with higher values during the interstadials of the D-O cycles (Fig. 3d). By contrast, cold periods of D-O cycles and HEs are characterized by lower abundance of alkenones. One exception to this pattern is observed during HE5, when abundance is the highest of the whole record.

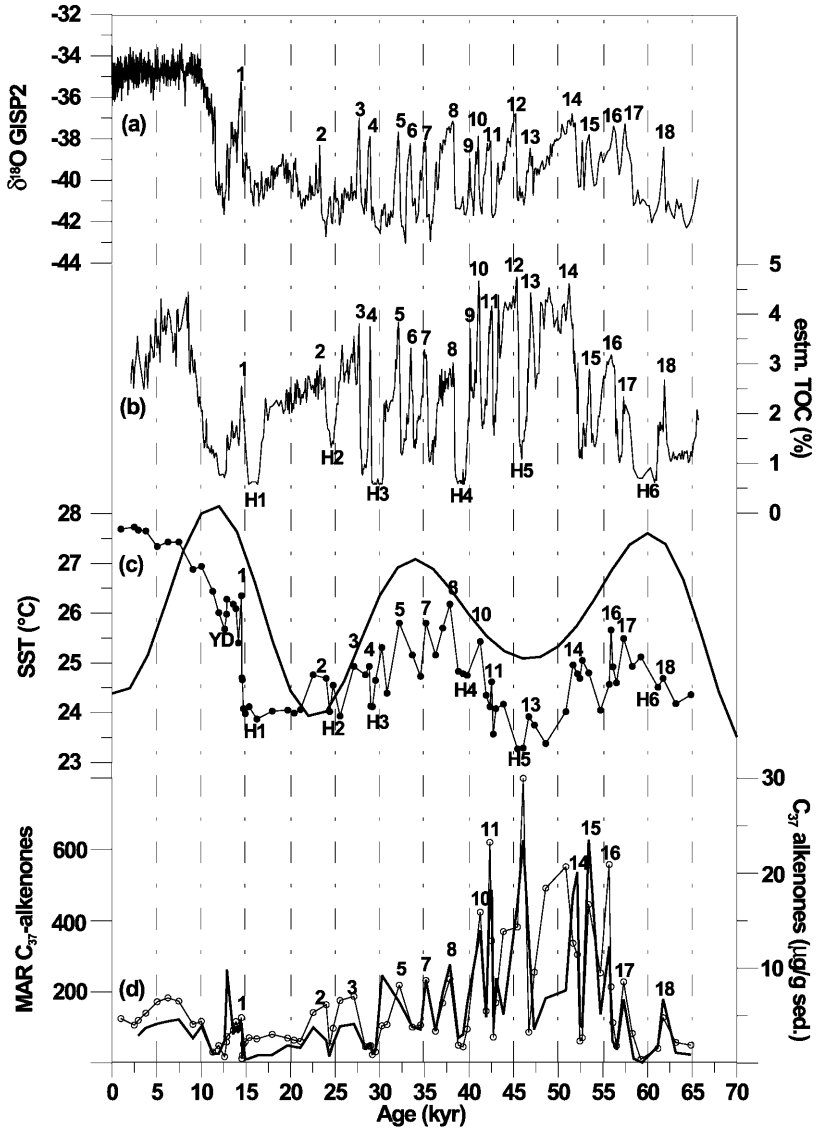

Fig. 3a–d Alkenone levels for core 136 KL, compared to the $\delta^{18}O$ record for the GISP2 ice core (Grootes et al. 1993) and the gray-scale-based TOC record for core 136 KL (Schulz et al. 1998). **a** $\delta^{18}O$ record for the GISP2 ice core. **b** Calculated gray-scale-based TOC record for core 136 KL. **c** Sea surface temperatures for core 136 KL (*closed circles*), estimated from $U^{k'}_{37}$-values of C_{37}-alkenones. The *line without circles* represents the insolation at 30°N (calculated after Berger 1978). **d** Contents of C_{37}-alkenones versus age (*thin line*), and mass accumulation rate (*MAR*) of alkenones (µg cm^{-2} 1,000 $year^{-1}$; *thick line*). The chronology of core 136 KL is based on $\delta^{18}O$ and AMS ^{14}C (Schulz et al. 1998 and personal communication). *Numbers* Dansgaard-Oescher events. *H1–H6* Heinrich events 1–6. *YD* Younger Dryas

Discussion

Sea surface temperatures

The observed temperature oscillations in core 136 KL are in good agreement with data derived from the Greenland $\delta^{18}O$ ice record in core GISP2 (Grootes et al. 1993; Fig. 3). Higher SSTs coincide with higher air temperature over Greenland during the interstadials of the D-O cycles. By contrast, stadials of the D-O cycles and Heinrich events (HE1–HE5) are characterized by lower SSTs in the Arabian Sea and cooler air temperatures over Greenland (Fig. 3a, c). The cooling during HE1–HE5 contradicts the results of numerical models, which simulated small positive SST anomalies in the Indian Ocean during comparative meltwater/control experiments (Manabe and Stouffer 1997; Schiller et al. 1997).

In the modern northeastern Arabian Sea lowest SSTs occur during the winter monsoon (Fig. 2e), and the magnitude of this surface water cooling seems to depend on wind speed (Almogi-Labin et al. 2000). In general SSTs reconstructed from alkenones in sediments represent annual mean temperatures of the surface mixed layer of the water column (e.g., Rostek et al. 1997; Müller et al. 1998). However, if the cold NE monsoon were to be stronger and/or longer than the warm SW monsoon, the annual mean temperature would decrease. We thus suggest that the lower temperatures (23–24 °C) recorded in core 136 KL during the cold periods of the D-O cycles and HEs may reflect an increase in the intensity and/or seasonal duration of the NE monsoon. This interpretation is consistent with the hypothesis of Porter and An (1995) who suggested (on the basis of grain-size variations) a stronger East Asian winter monsoon (which is coupled to the Indian Monsoon) during stadials of D-O cycles. Extreme deep winter mixing during HEs, as

invoked by Reichart et al. (1998), is also compatible with an enhancement of the NE monsoon. By contrast, during warm periods of the D-O cycles the annual mean SST may have been more influenced by the SW monsoon, comparable to modern conditions.

Long-term changes in insolation at 30°N seem to be superimposed on the millennial-scale SST fluctuations in the northeastern Arabian Sea during the last 65,000 years (Fig. 3c). This may explain the differences observed between the Greenland ice core and the SST record of core 136 KL. The YD in core 136 KL does not return to full glacial conditions, which is probably due to the insolation maximum at 30°N observed at the same time, which most likely counteracts the cooling of the YD. A similar mechanism could explain the relatively cold temperature observed during HE5 in core 136 KL, which coincides with an insolation minimum at 30°N. Such a surface water cooling at around 45 ka B.P. (so-called stage 3 event) was also observed in various cores from the western Arabian Sea (Zahn and Pedersen 1991; Caulet et al. 1992; Hermelin and Shimmield 1995), where it was interpreted as intensified, local, wind-induced upwelling (Hermelin and Shimmield 1995). Since there is no evidence for upwelling at location 136 KL, neither today nor in the past (Schulz et al. 1996, 1998; H. Schulz, personal communication), the observed temperature decrease can not be explained by enhanced upwelling. This extreme cooling is probably rather the result of the combination of enhanced NE monsoon and insolation minimum.

Paleoproductivity

Modern primary productivity at the location of core 136 KL is clearly coupled to the SW monsoon, as indicated by satellite observations (Antoine et al. 1996; Fig. 2). More recently it was further demonstrated that highest fluxes of alkenones occur in the Arabian Sea during the SW monsoon (Prahl et al. 2000; Fig. 2). Hence, C_{37}-alkenone abundance may be used as a proxy for the SW-monsoon intensity, with higher values indicating a stronger SW monsoon. This would imply that the SW monsoon was stronger during the interstadials of the D-O cycles, and weaker during the stadials of the D-O cycles and HEs. This interpretation is consistent with the results of marine records from the South China Sea, the Japan Sea and the Indian Ocean, evidently showing a weaker monsoon during the YD and H1 (Fang et al. 1999 and references therein). The interpretation of a stronger SW monsoon during the warm phases of the D-O cycles is in excellent agreement with the results from the western Chinese Loess Plateau (Fang et al. 1999), which also suggest stronger summer monsoons during the interstadials of the D-O cycles and weaker summer monsoons during the stadials of the D-O cycles and HEs (Fang et al. 1999). Evidently, alkenone enrichment can be used to evaluate the past SW-monsoon strength in the study area.

Accordingly, the high C_{37}-alkenone content observed in core 136 KL during HE5 implies that the SW monsoon was strengthened during this event, in contrast to all other HEs when the SW monsoon was weakened. At the China Loess location three different proxies (susceptibility, carbonate and soil color), which can be highly correlated with each other, were used by Fang et al. (1999) to evaluate summer-monsoon intensity. During HE5 a decoupling of susceptibility, carbonate and soil color was observed. The low carbonate content documented in the loess during HE5 (cf. Fang et al. 1999) indicates a strong summer monsoon with corresponding increase in precipitation. A stronger SW monsoon with enhanced primary productivity was also suggested by Hermelin and Shimmield (1995) in the northwestern Arabian Sea at around 45 ka B.P. (''stage 3'' event). In a sediment core obtained from the upwelling system of Socotra (NW Indian Ocean), a maximum of ''fertile'' Foraminifera was observed between 45 and 38 ka B.P., and was interpreted as an increase in paleoproductivity reflecting stronger upwelling activity (Vénec-Peyré and Caulet 2000). Enhanced alkenone and organic carbon levels around 45 ka B.P. in a sediment core of the upwelling area in the western Arabian Sea also point to an elevated primary productivity (Budziak et al. 2000). Thus, it seems likely that the maximum alkenone enrichment observed during H5 in core 136 KL indeed reflects a stronger SW monsoon in the study area at that time.

Teleconnection to North Atlantic climate

The good agreement between different geochemical records of cores 136 KL and GISP2 (Schulz et al. 1998; Schulte et al. 1999; this study) suggests that climatic changes in the Arabian Sea are phase locked with the rapid climatic changes recorded in Greenland ice cores. A coupling between North Atlantic and Arabian Sea climates has been suggested by several authors (e.g., Sirocko et al. 1996; Reichart et al. 1998), but the mechanism of coupling is still poorly understood.

A weakening of thermohaline circulation during the YD and HEs was demonstrated by several studies (e.g., Schiller et al. 1997; Vidal et al. 1997; Blunier et al. 1998). In the Arabian Sea, this in turn led to a further northwards expansion of oxygenated Antarctic intermediate water during the YD and HEs than is the case today. In contrast to the HEs, the thermohaline circulation during the warm periods of the D-O cycles was probably in its strong mode, with an intermediate-depth hydrography comparable to modern conditions (Schulte et al. 1999). Apparently, the development of the OMZ in the Arabian Sea is coupled to the North Atlantic climate via thermohaline circulation.

Our results clearly indicate that winter/summer-monsoon strength changed in concert with high-frequency and large-amplitude fluctuations of the North Atlantic climate, which is in good agreement with other

studies (Porter and An 1995; Sirocko et al. 1996; Fang et al. 1999). Changes in continental surface and air conditions, and thus in atmospheric circulation, would be the most likely mechanism to explain this teleconnection.

The Tibet Plateau has played a major role in adjusting Asian and Northern Hemisphere atmospheric circulation (Ruddiman and Kutzbach 1989; Kutzbach et al. 1989). Numerical modeling demonstrates that uplift of the Tibet Plateau in the late Cenozoic not only generated the monsoon (Ruddiman and Kutzbach 1989) but also strengthened the Westerlies, which act as a "wall" to hinder heat exchange between the Equator and high latitudes (Kutzbach et al. 1989). It was shown that the Tibet low, which develops in summer, considerably changes the strength of the summer monsoon, and that changes in position and strength of the Westerlies also greatly affect the summer monsoon (Ruddiman and Kutzbach 1989; Kutzbach et al. 1989). A Westerlies-swinging model was proposed by Fang et al. (1999) to explain the enhanced summer monsoon during the interglacials and interstadials of the D-O cycles, caused by a strong Tibet low and a shifting of the Westerlies towards the north. By contrast, weakened summer monsoons during glacials and HEs were explained by a reduced Tibet low and southward-moving Westerlies (Fang et al. 1999). Westerlies are intensified and may shift south of the Tibet Plateau even in summer during times when polar and North Atlantic cold air surges cause an expansion of the winter monsoon and a fast drop of the summer monsoon. Such a scenario would be consistent with the results of an ocean-atmosphere general circulation model which simulated stronger Westerlies during a meltwater experiment (Schiller et al. 1997). Hence, weakening of the thermohaline circulation and degree of heat supply in the North Atlantic substantially influences the monsoon through the Westerlies (Fang et al. 1999). Evidently, the Arabian Sea is teleconnected to the North Atlantic climate via not only oceanic but also atmospheric circulation.

Conclusions

The SST record of core 136 KL shows striking similarities with the $\delta^{18}O$ record of Greenland ice core GISP2. Apparently, variations of SST in the northeastern Arabian Sea reflect changes in NE-monsoon strength. During the cold periods of the D-O cycles and Heinrich events, the NE monsoon was strengthened which resulted in lower SSTs. By contrast, the warm periods of the D-O cycles are characterized by higher SSTs and weakened NE monsoons.

Primary productivity was high during the interstadials of D-O cycles, implying stronger SW monsoons. By contrast, the stadials of D-O cycles and HEs are characterized by lower productivity, indicating a weaker SW monsoon during these intervals. HE-5 is an exception to this pattern, exhibiting high productivity pointing to a stronger SW monsoon. This productivity event at around 45 ka B.P. was also reported in other sediment cores from the western Arabian Sea, and may be a local phenomenon (Hermelin and Shimmield 1995; Vénec-Peyré and Caulet 2000; Budziak et al. 2000).

The North Atlantic climate signal is connected to the Arabian Sea by the Westerlies, which in turn are influenced by heat transport to the high latitudes driven by the thermohaline circulation. Thus, the two regions are teleconnected by both oceanic and atmospheric circulation.

Acknowledgements We thank Jürgen Rullkötter (ICBM, Oldenburg, Germany), Ulrich von Rad and Heidi Doose-Rolinski (BGR, Hannover, Germany) for providing samples. We are also grateful to Ralf Kreutz for analytical assistance and to Carsten Rühlemann for useful suggestions. Reviews by Andreas Lückge and an anonymous reviewer are greatly appreciated. Data are available in the world data center PANGAEA (http://www.pangaea.de/home/sschulte).

References

Almogi-Labin A, Schmiedl G, Hemleben C, Siman-Tov R, Segl M, Meischner D (2000) The influence of the NE winter monsoon on productivity changes in the Gulf of Aden, NW Arabian Sea, during the last 530 ka as recorded by Foraminifera. Mar Micropaleontol 40:295–319

Andruleit HA, von Rad U, Bruns A, Ittekkot V (2000) Coccolithophore fluxes from sediment traps in the northeastern Arabian Sea off Pakistan. Mar Micropaleontol 38:285–308

Antoine D, André JM, Morel A (1996) Oceanic primary production. 2. Estimation at global scale from satellite (coastal zone color scanner) chlorophyll. Glob Biogeochem Cycles 10:57–69

Banse K (1984) An overview of the hydrography and associated biological phenomena in the Arabian Sea, off Pakistan. In: Haq BU, Milliman JD (eds) Marine geology and oceanography of the Arabian Sea and coastal Pakistan. Van Nostrand Reinhold, New York, pp 271–304

Banse K (1994) On the coupling of hydrography, phytoplankton, zooplankton, and settling organic particles offshore in the Arabian sea. In: Lal D (ed) Biogeochemistry in the Arabian Sea. Proc Indian Acad Sci, Earth Planet Sci 103:125–161

Bard E (2001) Comparison of alkenone estimates with other paleotemperature proxies. Geochem Geophys Geosyst G3, Pap No 2000GC000050

Bard E, Rostek F, Turon J-L, Gendreau S (2000) Hydrological impact of Heinrich events in the subtropical northeast Atlantic. Science 289:1321–1324

Bearman G (ed) (1991) Ocean circulation. Pergamon, Oxford

Behl RJ, Kennett JP (1996) Brief interstadial events in the Santa Barbara basin, NE Pacific, during the past 60 kyr. Nature 379:243–246

Bender M, Sowers T, Dickson M-L, Orchado J, Grootes PM, Mayewski PA, Messe DA (1994) Climate correlations between Greenland and Antarctica during the last 100,000 years. Nature 372:663–666

Benthien A, Müller PJ (2000) Anomalously low alkenone temperatures caused by lateral particle and sediment transport in the Malvinas Current region, western Argentine Basin. Deep-Sea Res I 47:2369–2393

Berger AL (1978) Long-term variations of daily insolation and Quaternary climate change. J Atmos Sci 35:2362–2367

Blunier T, Chappelaz J, Schwander J, Dällenbach A, Stauffer B, Stocker TF, Raynaud D, Jouzel J, Clausen HB, Hammer CU, Johnson SJ (1998) Asynchrony of Antarctic and Greenland climate change during the last glacial period. Nature 394:739–743

Bond GC, Broecker WS, Johnson SJ, McManus JF, Labeyrie L, Jouzel J, Bonani G (1993) Correlations between climate records from North Atlantic sediments and Greenland ice. Nature 365:143–147

Brassell SG, Eglinton G, Marlowe IT, Pflaumann U, Sarnthein M (1986) Molecular stratigraphy: A new tool for climatic assessment. Nature 320:129–133

Brock JC, McClain CR, Anderson DM, Prell WL, Hay WW (1992) Southwest monsoon circulation and environments of recent planktonic Foraminifera. Paleoceanography 7:799–813

Budziak D, Schneider RR, Rostek F, Müller PJ, Bard E, Wefer G (2000) Late Quaternary insolation forcing on total organic carbon and C_{37} alkenone variations in the Arabian Sea. Paleoceanography 15:307–321

Cacho I, Grimald JO, Pelejero C, Canals M, Sierro FJ, Flores JA, Shackleton N (1999) Dansgaard-Oeschger and Heinrich event imprints in Alboran Sea paleotemperatures. Paleoceanography 14:698–705

Caulet JP, Vénec-Peyré M-T, Vergnaud-Grazzini C, Nigrini C (1992) Variations of South Somalia upwelling during the last 160 ka: Radiolarian and Foraminifera records in core MD 85674. In: Summerhayes CP, Prell WL, Emeis KC (eds) Upwelling systems: evolution since the early Miocene. Geol Soc Lond Spec Publ 64:379–389

Clemens S, Prell WL, Murray D, Shimmield G, Weedon G (1991) Forcing mechanisms of the Indian monsoon. Nature 353:720–725

Conte MH, Eglinton G (1993) Alkenone and alkenoate distributions within the euphotic zone of the eastern North Atlantic: correlation with production temperature. Deep-Sea Res I 40:1935–1961

Dansgaard W, Johnsen SJ, Clausen HB, Dahl-Jensen D, Gundestrup NS, Hammer CU, Hvidberg CS, Steffensen JP, Sveinbjörnsdottir AE, Jouzel J, Bond G (1993) Evidence for general instability of past climate from a 250 kyr ice-core record. Nature 364:218–220

Doose-Rolinski H, Rogalla U, Scheeder G, Lückge A, von Rad U (2001) High-resolution temperature and evaporation changes during the late Holocene in the northeastern Arabian Sea. Paleoceanography 16:358–367

Fang X-M, Ono Y, Fukusawa H, Bao-Tian P, Li J-J, Dong-Hong G, Oi K, Tsukamoto S, Torii M, Mishima T (1999) Asian summer monsoon stability during the past 60,000 years: magnetic susceptibility and pedogenic evidence from the western Chinese Loess Plateau. Earth Planet Sci Lett 168:219–232

Grootes PM, Stuiver M, White JWC, Johnsen S, Jouzel J (1993) Comparison of oxygen isotope records from the GISP2 and GRIP Greenland ice cores. Nature 366:552–554

Heinrich H (1988) Origin and consequences of cyclic ice rafting in the northeast Atlantic Ocean during the past 130,000 years. Quat Res 29:143–152

Hermelin JOR, Shimmield GB (1995) Impact of productivity events on the benthic foraminiferal fauna in the Arabian Sea over the last 150,000 years. Paleoceanography 10:85–116

Johnsen SJ, Clausen HB, Dansgaard W, Fuhrer K, Gundestrup N, Hammer CU, Iversen P, Jouzel J, Stauffer B, Steffensen JP (1992) Irregular glacial interstadials recorded in a new Greenland ice core. Nature359:311–313

Kutzbach JE, Gueter PJ, Ruddiman WF, Prell WL (1989) Sensitivity of climate to late Cenozoic uplift in southern Asia and the American West: numerical experiments. J Geophys Res 94(D15):18393–18407

Leuschner DC, Sirocko F (2000) The low-latitude monsoon climate during Dansgaard-Oeschger cycles and Heinrich events. Quat Sci Rev 19:243–254

Lin H-L, Lai C-T, Ting H-C, Wang L, Sarnthein M, Hung J-J (1999) Late Pleistocene nutrients and sea surface productivity in the South China Sea: a record of teleconnection with Northern hemisphere events. Mar Geol 156:197–210

Madhupratap M, Prasanna Kumar S, Bhattathiri P, Dileep Kumar M, Raghukumar S, Nair K, Ramaiah N (1996) Mechanism of the biological response to winter cooling in the northeastern Arabian Sea. Nature 384:549–551

Manabe S, Stouffer FJ (1997) Coupled ocean-atmosphere model response to freshwater input: comparison to Younger Dryas event. Paleoceanography 12:321–336

Müller PJ, Kirst G, Ruhland G, von Storch I, Rosell-Melé A (1998) Calibration of the alkenone paleotemperature index $U^{k'}_{37}$ based on core-tops from the eastern South Atlantic and the global ocean (60°N–60°S). Geochim Cosmochim Acta 62:1757–1772

Olson DB, Hitchcock GL, Fine RA, Warren BA (1993) Maintenance of the low-oxygen layer in the central Arabian Sea. Deep-Sea Res 40:673–685

Pickard GL, Emery WJ (1982) Descriptive physical oceanography, an introduction, 4th edn. Pergamon, Oxford

Porter SC, An Z (1995) Correlation between climate events in the North Atlantic and China during the last glaciation. Nature 375:305–308

Prahl FG, Dymond J, Sparrow MA (2000) Annual biomarker record for export production in the central Arabian Sea. Deep-Sea Res 47:1581–1604

Reichart GJ, Lourens LJ, Zachariasse WJ (1998) Temporal variability in the northern Arabian Sea oxygen minimum zone (OMZ) during the last 225,000 years. Paleoceanography 13:607–621

Rostek F, Bard E, Beaufort L, Sonzogni C, Ganssen G (1997) Sea surface temperature and productivity records for the past 240 kyr in the Arabian Sea. Deep-Sea Res II 44:1461–1480

Ruddiman WF, Kutzbach JE (1989) Forcing of late Cenozoic Northern Hemisphere climate by plateau uplift in Southern Asia and the American West. J Geophys Res 94(D15):18409–18427

Rühlemann C, Mulitza S, Müller PJ, Wefer G, Zahn R (1999) Warming of the tropical Atlantic Ocean and slowdown of thermohaline circulation during the last deglaciation. Nature 402:511–514

Schiller A, Mikolajewicz U, Voss R (1997) The stability of the thermohaline circulation in a coupled ocean-atmosphere general circulation mode. Climate Dyn 13:325–348

Schubert CJ, Villanueva J, Calvert SE, Cowie GL, von Rad U, Schulz H, Berner U, Erlenkeuser H (1998) Stable phytoplankton community structure in the Arabian Sea over the past 200,000 years. Nature 394:563–566

Schulte S, Rostek F, Bard E, Rullkötter J, Marchal O (1999) Variations of oxygen-minimum and primary productivity recorded in sediments of the Arabian Sea. Earth Planet Sci Lett 173:205–221

Schulz H, von Rad U, von Stackelberg U (1996) Laminated sediments from the oxygen minimum zone of the northeastern Arabian Sea. In: Kemp AES (ed) Paleoclimatology and paleoceanography from laminated sediments. Geol Soc Lond Spec Publ 116:185–207

Schulz H, von Rad U, Erlenkeuser H (1998) Correlation between Arabian Sea and Greenland climate oscillations of the past 110,000 years. Nature 393:54–57

Sirocko F, Garbe-Schönberg D, McIntyre A, Molfino B (1996) Teleconnections between the subtropical monsoons and high-latitude climates during the last deglaciation. Science 272:526–529

Sonzogni C, Bard E, Rostek F (1998) Tropical sea-surface temperatures during the last glacial period: a view based on alkenones in Indian Ocean sediments. Quat Sci Rev 17:1185–1201

Swallow JC (1984) Some aspects of the physical oceanography of the Indian Ocean. Deep-Sea Res 31:639–685

Thouveny N, de Beaulieu J-L, Bonifay E, Creer KM, Guiot J, Icole M, Johnsen SJ, Jouzel J, Reille M, Williams T, Williamson D (1994) Climate variations in Europe over the past 140 kyr deduced from rock magnetism. Nature 371:503–506

Vénec-Peyré M-T, Caulet J-P (2000) Paleoproductivity changes in the upwelling system of Socotra (Somali Basin, NW Indian Ocean) during the last 72,000 years: evidence from biological signatures. Mar Micropaleontol 40:321–344

Vidal L, Labeyrie L, Cortijo E, Arnold M, Duplessy JC, Michel E, Becqué S, van Weering TCE (1997) Evidence for changes in the North Atlantic Deep Water linked to meltwater surges during the Heinrich events. Earth Planet Sci Lett 146:13–27

Villanueva J, Grimalt JO, Labyrie LD, Cortijo E, Vidal L, Turon J-L (1998) Precessional forcing of productivity in the North Atlantic Ocean. Paleoceanography 13:561–571

Volkman JK, Barrett SM, Blackburn SI, Sikes EL (1995) Alkenones in *Gephyrocapsa oceanica:* implications for studies of paleoclimate. Geochim Cosmochim Acta 59:513–520

von Rad U, Schulz H, SONNE 90 Scientific Party (1995) Sampling the oxygen minimum zone off Pakistan: glacial-interglacial variations of anoxia and productivity (preliminary results, SONNE 90 cruise). Mar Geol 125:7–19

Wang L, Sarnthein M (1999) Long-/short-term variations of monsoon climate and its teleconnection to global change. In: Abrantes F, Mix A (eds) Reconstructing ocean history: a window into the future. Plenum, New York, pp 57–71

Wyrtki K (1973) Physical oceanography of the Indian Ocean. In: Zeitschel B (ed) The biology of the Indian Ocean. Springer, Berlin Heidelberg New York, pp 18–36

Zahn R, Pedersen TF (1991) Late Pleistocene evolution of surface and mid-depth hydrography at the Oman margin: planktonic and benthic isotope records at site 724. In: Prell WL et al (eds) Proceedings of the Ocean Drilling Program, Scientific Results, Leg 117. College Station, Texas, pp 291–308

Zhou W, Head MJ, Lu X, An Z, Jull AJT, Donahue D (1999) Teleconnection of climatic events between East Asia and polar, high latitude areas during the last deglaciation. Palaeogeogr Palaeoclimatol Palaeoecol 152:163–172